Fat Particle Structure and Stability of Food Emulsions

WEN XU, ALEX NIKOLOV, DARSH T. WASAN, ALEX GONSALVES, and RAJENDRA P. BORWANKAR

ABSTRACT

We used a nondestructive Kossel diffraction technique based on the principle of backlight scattering to characterize the structure formation in concentrated model food emulsions. We also measured the effects of temperature, shear, casein micelles and gum on the fat particle packing structure in such systems. Through this technique, we demonstrated the effects of casein micelles on the pair potential of fat particle interactions and shelf life of such systems. We carried out theoretical calculations using a statistical mechanics approach by numerically solving the Ornstein-Zernike equation with Percus-Yevick closure for a bidisperse system consisting of fat particles and micelles, and showed that the experimental results were consistent with theoretical simulations.

Key Words: particle structure, emulsion stability, light scattering, caseinate, gum, shear rate

INTRODUCTION

AS WITH MOST COLLOIDAL SYSTEMS, THE *INTERACTIONS* BEtween fat particles inside food emulsions are very important in the stability and texture of products. They may determine the rheological properties and the appearance of the product, as well as its physical instability, as reflected in changes of consistency or loss of homogeneity (Walstra, 1993).

Many factors, such as protein concentration, gum, temperature, shear rate, fat particle concentration and polydispersity, and nonadsorbed particles, may affect fat particle interactions and the stability of food emulsions. Koczo et al. (1996) reported a stability mechanism for food emulsions due to the microlayering of sodium caseinate submicelles in the thin liquid films between fat particles. The existence of the submicelle layers in the thin liquid films between fat particles prevented fat particles from approaching each other, thus stabilizing the food emulsions. Creaming (flocculation) of a model food emulsion in the presence of xanthan and guar gums was then studied (Koczo et al., 1997). The mechanism of dispersion separation by xanthan gum was a geometrical incompatibility between the anisotropic, wormlike-chain shaped xanthan molecules and the isotropic dispersed fat particles.

Particle structure variations under shear stress have been investigated by Ackerson and Clark (Ackerson and Clark, 1981). They found that when the dispersions of charged spherical colloidal particles were subjected to an increasing shear rate, the particle structure exhibited a reversible and order-disorder transition and became an amorphous structure at high shear rate. Effects of particle concentration and polydispersity on the particle interactions in colloidal dispersions have been studied theoretically (Chu et al., 1996) and experimentally (Xu et al., 1997). In a near hard sphere system, due to the increase of the particle concentration, the particle packing structure was found to become more ordered and both structural energy barrier and depletion increased, while the particle packing structure became less ordered when the particle polydispersity increased.

The fat particle packing structure inside whipped cream was studied by Brooker (Brooker et al., 1986; Brooker, 1990; Anderson and Brooker, 1988) using transmission and scanning electron microscopy. Qualitative information about the particle packing structure in the bulk phase was reported. Much information about the fat particle packing structure has been qualitative due to the lack of measurement methods and complexity of food systems. The effects of interparticle interactions on the stability of food emulsions are not understood.

Our main objective was to generate a quantitative description of the fat particle structure using backlight scattering technique, and to understand the effects of fat particle-particle interactions in the stability of food emulsions. The effects of protein submicelles, temperature, gum (xanthan) and shear rate on the fat particle structuring and the stability of food emulsions were investigated.

THEORY

Light scattering theory

Light scattering is one technique to obtain structural and thermodynamic information about dispersions. For a monodisperse system of spherically symmetric particles, when the particle size is slightly smaller than the incident polarized light wavelength, Rayleigh-Gan-Debye theory (Hunter, 1987) can be applied,

$$I(Q) = ANP(Q)S(Q) \quad (1)$$

where I(Q) is the intensity of the scattered light at a scattering vector Q, A is a normalized constant that can be determined by the requirement (Nieuwenhuis and Vrij, 1979) that

$$\int_0^\infty Q^2[S(Q) - 1]dQ = 2\pi^2 N \quad (2)$$

where N is the particle number density, P(Q) is the form factor which is a property of particle shape and size, and can be obtained from light scattering experiment of dilute colloidal dispersions,

$$S(Q)_{\phi\text{-}0} = 1 \quad (3)$$

and

$$P(Q) = [I(Q)_{\phi\text{-}0}] / (A^*N^*) \quad (4)$$

where ϕ is the particle volume fraction, A^* is an unknown constant, and N^* is the particle number density of dilute colloidal dispersions. In this experiment, the fat concentration of food emulsions to infer the form factor was around 0.1 vol%.

Then the static structure factor S(Q) could be determined from the following equation,

$$S(Q) = [(A^*N^*) / AN] [I(Q) / I(Q)_{\phi\text{-}0}] \quad (5)$$

where S(Q) is the static structure factor which describes the degree of particle structure ordering inside colloidal dispersions. We had found (Xu et al., 1997) that the higher the first peak of the static structure factor, the more ordering there was in the particle packing structure. The typical range of the first peak height for common food colloidal systems is around 1 to 3. $[A^*N^*/AN]$ is a constant, which can be determined by Eq. (2). Q is the scattering vector that is defined by

Authors Xu, Nikolov and Wasan are with the Chemical Engineering Dept., Illinois Institute of Technology, Chicago, IL 60616. Authors Gonsalves and Borwankar are with Kraft Foods, Glenview, IL 60025. Address inquiries to Dr. D.T. Wasan.

$$Q = (4\pi/\lambda)\sin(\theta/2) \quad (6)$$

where θ is the scattering angle.

The radial distribution function g(r) which measures the probability to find a particle center at a distance r from a given particle can be calculated from the experimental value of S(Q) by the Fourier transform (Mandel, 1971),

$$g(r) = 1 + (1/(2\pi^2 Nr)\int_0^\infty [S(Q) - 1)Q \sin(Qr)dQ \quad (7)$$

and the average pair potential (potential of mean force), which is the potential (free) energy of a pair in the presence of the other particles, can be calculated from the radial distribution function g(r) (Hunter, 1987),

$$U(r) = kT\ \lng(r) \quad (8)$$

For a polydisperse system, the structure factor can be obtained directly by straightforward generalization of Equation (1) to the case of p nonidentical particles (D'Aguanno and Klein, 1991),

$$<I(Q)> = NA'P'(Q)S^M(Q) \quad (9)$$

where the quantities A' and P'(Q) are given by the averages over the particle type distribution,

$$A' = \sum_{\alpha=1}^{p} x_\alpha A_\alpha \quad (10)$$

and

$$P'(Q) = (1/A')\sum_{\alpha=1}^{p} x_\alpha A_\alpha P_\alpha(Q) \quad (11)$$

where *x* is the molar fraction of the species α. The structure factor, $S^M(q)$ is defined by

$$S^M(Q) = 1/[A'P'(Q)]\sum_{\alpha=1}^{p}\sum_{\beta=1}^{p}[A_\alpha A_\beta P_\alpha(Q)P_\beta(Q)]^{1/2}S_{\alpha\beta}(Q) \quad (12)$$

As with the monodisperse system, the average form factor P'(Q) could be obtained from the light scattering experiment of dilute (noninteraction) colloidal dispersions,

$$P'(Q) = [<I(Q)>_{\phi\text{-}0}] / (A'N) \quad (13)$$

Note that although there were conceptual differences between $S^M(Q)$ and the corresponding S(Q) for the monodisperse system (for example, the meaning of S(Q=0) and the first peak position Q_{max}, etc.), the variation trend of the first main peak height as a function of polydispersity was the same while the total volume fraction was kept constant. Also the differences of the main peak height between the measured structure factor $S^M(Q)$ and the Bhatla-Thornton structure factor or S (Q), known to better represent the particle microstructure of a polydisperse system, was very small (D'Aguanno and Klein, 1991). Therefore, the main peak height $S^M(Q)$ could still be used to approximate the particle microstructure of a polydisperse system.

Theoretical model of interparticle interactions in bidisperse colloidal systems

According to Eq. (7) and (8), the particle structure and particle-particle interactions inside colloidal systems could be determined from the radial distribution function g(r). Therefore, it was necessary to theoretically calculate this radial distribution function. A hard sphere was assumed and the interparticle potential for a monodisperse system could then be represented as

$$V(r) = \begin{cases} \infty, & r<d \\ 0, & r>d \end{cases} \quad (14)$$

where d is the particle diameter.

The Ornstein-Zernike (1914) (O-Z) theory was employed to calculate the correlation function in a many body system. It states that the total correlation function h(r), which is related to the radial distribution function g(r) by h(r) = g(r)-1, consists of two parts. The first is the direct correlation between the two particles, denoted by c(r), and the second is contributed by all possible indirect correlations through the other particles in the system. The indirect correlations can be expressed exactly as the convolution of the direct correlation function and the total correlation function.

The above explanation can be expressed by the O-Z integral equation,

$$h(r) = c(r) + N\int h(|r\text{-}z|)c(z)dz \quad (15)$$

where is the particle number density.

In order to solve the O-Z equation, an appropriate closure relation between the two correlation functions is needed. The Percus-Yevick equation (Percus and Yevick, 1957)

$$[h(r) + 1][1–\exp(V(r)/kT] = c(r) \quad (16)$$

is most widely used for hard sphere systems.

For a binary mixture of hard spheres, the bare pair interaction between two hard sphere particles becomes

$$V(r)_{ij} = \begin{cases} \infty, & r<d_{if} \\ O, & r>d_{ij} \end{cases} \quad (17)$$

where $d_{ij} = (d_i + d_j)/2$ is the center-to-center distance between particle i and particle j when they are in contact.

Similar to a monodisperse system, the O-Z integral equation also can be used to express the particle-particle interaction in a binary mixture system,

$$h_{ij}(r_{12}) = c_{ij}(r_{12}) = \sum_{l=1}^{2}\int N_l\, h_{ij}(r_{13})c_{i\,j}(r_{32})dr_3 \quad (18)$$

where N_l is the density of particle type l, C_{ij} is the direct correlation between particles i and j, and h_{ij} is the total correlation function between particles i and j.

In order to solve the above O-Z equation, an appropriate closure relation between the two correlation functions $h_{ij}(r)$ and $C_{ij}(r)$ was needed. A generalized Percus-Yevick equation (Percus and Yevick, 1957) for mixtures was used in this model,

$$[h_{ij}(r) + 1][1\text{-}\exp(V_{ij}(r)/k'T)] = c_{ij}(r) \quad (19)$$

The exact solution of the generalized O-Z equation was derived by Lebowitz (1964), where

$$g_{ij}(r) = \frac{1}{12(\eta_i\eta_j)^{1/2}r}\Omega^{-1}[G_{ij}(S)] \quad (20)$$

where

$$G_{11}(s) = s[h\text{-}L_2(s)e^{sd_2}]/D(s)$$

$$G_{12}=G_{21}=(\eta_1\eta_2)^{1/2}s^2e^{sR_{12}}[\tfrac{3}{4}(\eta_2R_2^3-\eta_1R_1^3)R_2-R_1)-R_{12}(1+\tfrac{1}{2}\xi)]s-(1+2\xi)/D(s)$$

$$D(s)=h-L_1(s)e^{sd_1}-L_2(s)e^{sd_2}+S(s)e^{s(d_1+d_2)}$$

$$S(s)=h+[12(\eta_1+\eta_2)(1+2\zeta)-h(d_1+d_2)]s$$
$$-18(\eta_1 d_1^2+\eta_2 d_2^2)^2 s^2-6(\eta_1 d_1^2+\eta_2 d_2^2)(1-\zeta)s^3-(1-\zeta)^2 s^4$$

$$L_1(s) = 12\eta_2[(1+(½\zeta) + (3/2)\eta_1 d_1^2(d_2-d_1)]d_2 s^2 +[12\eta_2(1+2\zeta)-hd_1]s+h$$

$$h = 36\eta_1\eta_2(d_2-d_1)^2$$

$$\eta_i = \pi N_i/6$$

$$\zeta = \eta_1 d_1^3 + \eta_2 d_2^3$$

and $G_{22}(s)$, $L_2(s)$ can be found from $G_{11}(s)$ and $L_1(S)$ by interchanging $_1$, R_1 with $_2$, R_2.

In our research, Eq. (1) through (6), and (9) through (13) were used to calculate static structure factors, while Eq. (7), (8), and (14) through (20) were used to calculate pair potentials of mean force.

MATERIALS & METHODS

Materials

The emulsion preparation is as follows: Sodium caseinate, emulsifiers (polysorbate 60 and sorbitan monostearate) and gums (xanthan and guar) were dispersed in water. Partially hydrogenated vegetable oil, syrups, and flavors were then added to make a pre-emulsion, which was then pasteurized and homogenized in a 2-stage homogenizer. The resulting emulsion was cooled to 1–3°C and aged for 45 min in a tank at about 5°C to produce the final emulsion samples used in this study. Four model food emulsion samples were prepared by this method (Table 1).

The fat particle size distributions (Fig. 1) inside food emulsion samples were measured using a Horiba LA-900 particle size distribution analyzer (Horiba Instruments Incorporated, Irvine, California). The fat particle size distribution inside all 4 food emulsion samples was nearly the same.

Table 1—Main composition of the food emulsions

Sample	Fat (wt%)	Caseinate (wt%)	Polysorbate60 (wt%)	Xanthan (wt%)
#1	5.14	0.48	0.00	0.00
#2	5.14	0.00	0.33	0.00
#3	5.14	0.48	0.00	0.16
#4	5.14	0.24	0.00	0.00

Backlight scattering experiment

The backlight scattering measurements were carried out using a system we developed (Fig. 2). A collimated green light beam (50 m dia, wavelength 543 nm) produced by a 0.5 mw He-Ne Laser (Model 155A, Spectra-Physics Laser Products, Mountain View, CA) was scattered by colloidal particles inside the sample with controlled temperature, and produced a scattering image on the surface of a glass vial. The image intensity was then recorded by a vertically polarized CCD digital camera (Lynxx 2000 Frame 336*244FT, Spectra Source Instruments, Westlake Village, CA) and down loaded to a connected computer (IBM compatible PC Pentium/120 Mhz). The recorded image was transformed to an intensity profile by image analyzer software (Spectra Source Instrument - Lynxx 2000 Version 3.04b, Westlake, CA). An experimental backlight scattering image of sample #1 at a temperature of °C is shown (Fig. 3) as well as the corresponding backlight scattering intensity profile (Fig. 4).

Fat particle structure study inside food emulsions under shear

In this experiment, a concentric cylinder cell was used (Fig. 5) in

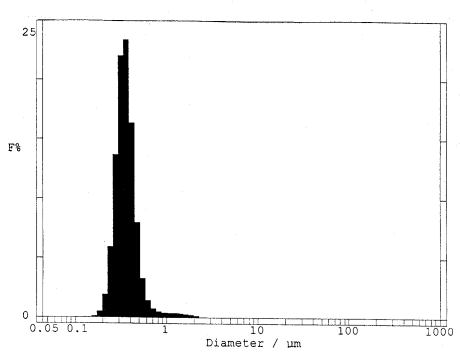

Fig.1—Particle size distribution of sample #1 measured by Horiba LA-900 particle size distribution analyzer.

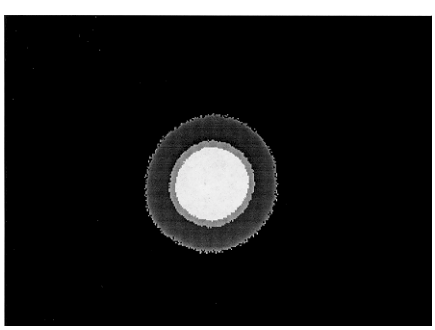

Fig. 3—Backlight scattering image of sample #1 at 5°C.

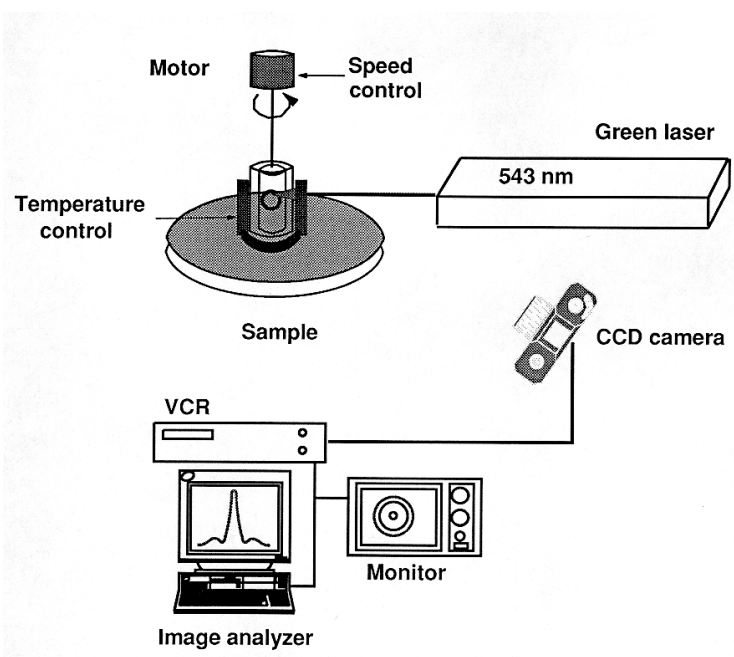

Fig. 2—Back-light scattering experimental set-up.

which the inner cylinder rotated to produce a nearly uniform steady-state shear rate on the food emulsion sample. The shear rate could be changed by controlling the rotation speed of the inner cylinder, and the sample temperature was kept at °C during the shear experiment.

RESULTS & DISCUSSION

Effect of sodium caseinate

Sodium caseinate is commonly used in the food industry as an emulsion and foam stabilizer. In order to study the effects of caseinate on fat particle structure, a backlight scattering experiment was carried out (Fig. 6). The two samples included the same fat concentration (5.14 wt% fat) except that the caseinate concentration inside sample #4 was half of that inside sample #1. The first peak height of the structure factor $S(Q)_{max}$ of the sample with higher caseinate concentration was higher, indicating that the addition of caseinate facilitated the fat particle structure formation. This could be explained by the stabilization mechanism of caseinate submicelles in the aqueous phase. When the submicelle concentration exceeds a critical value, they can form a layer structure around the fat particles (Koczo et al., 1996), which has a stabilization effect on the emulsion.

Results for a binary system were calculated (Fig. 7) from the O-Z method. The parameters used in this calculation were D_{large}/d_{small} = 20 and the volume fraction of large particles equal to 5 vol%. We observed that with the small particle concentration increasing, the structure energy barrier between large particles increased rapidly. When the small particle concentration reached 20 vol%, the structure energy barrier was much larger than 3 kT. Such a high energy barrier was enough to prevent the large particle aggregation, therefore, the emulsion became more stable.

In the sample #1, the caseinate submicelle concentration was estimated to be around 15 ~ 20 vol% (Koczo, et al., 1996), therefore, this microlayering stabilization mechanism went into effect. Another contribution to the emulsion stability by caseinate resulted from the adsorption of caseinate on the fat/water interface (Dickinson and Stainsby, 1988; Dickinson, 1992; Dickinson and Walstra, 1993).

Effect of xanthan

The low surface activity of xanthan requires that it is rarely used alone as an emulsifying or foaming agent, although it is often used

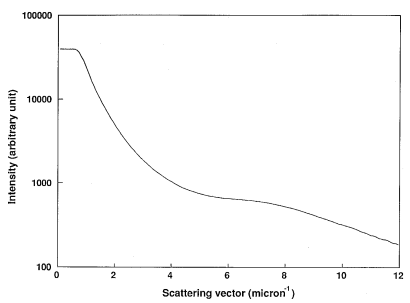

Fig. 4—Back-light scattering intensity profile of sample #1 at 5°C.

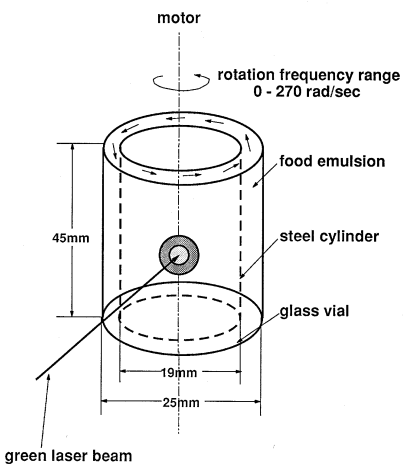

Fig. 5—Experimental set-up to study the effect of shear rate on food emulsion stability.

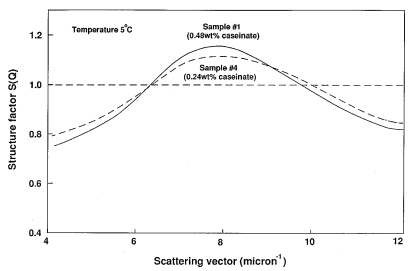

Fig. 6—Effect of caseinate on fat particle structure inside food emulsions (fat concentration: 5.14 wt%).

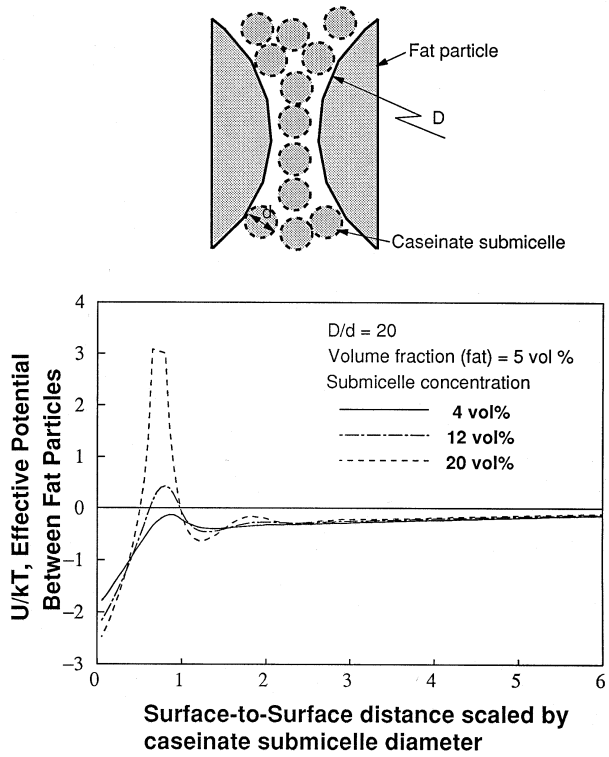

Fig. 7— Stabilization mechanism of caseinate submicelle microlayering: calculation results from O-Z method (particle size ratio: 20 & fat concentration: 5 vol%).

as an emulsion and foam stabilizer. Addition of xanthan greatly increases the bulk viscosity, and thus the stability and texture of food emulsions and foams are improved.

The destabilizing effect of xanthan is related to the strongly anisotropic character of xanthan macromolecules. According to the Flory (Flory, 1956; Flory and Abe, 1978) theory, a dispersion including anisotropic particles tends to separate. In an isotropic phase the anisotropic particle concentration is lower and the orientation of the particles is random. In another anisotropic phase the particles have similar orientations. The phase separation in such systems starts when the axis (l/dia) ratio of the particles is 5.4 and the separation becomes more pronounced with increasing particle axis ratio. For the xanthan molecule, the axis ratio is much lager than 5.4 (Koczo et al., 1996), therefore, phase separation occurs.

The effects of xanthan on fat particle structure were determined experimentally (Fig. 8). These two samples included the same ingredients except that one sample (#3) included xanthan (0.16 wt%) and the other (#1) had no xanthan. The peak height of the sample without xanthan was much higher than that of the other sample, indicating that existence of anisotropic xanthan macromolecules made the fat particle packing structure much less ordered. As a consequence, the fat particle structure inside the food emulsion was destroyed.

Effect of temperature

The effect of temperature was determined (Fig. 9) on the fat particle static structure. Here the Y axis was the normalized structure factor defined as $S(Q)_{max}/S(Q)_{min}$, where $S(Q)_{max}$ was the first peak height, and $S(Q)_{min}$ was the value of structure factor at the minimum position after the first peak. The two samples had the same fat particle concentration (5.14 wt%) except that one sample (#1) was caseinate-stabilized and the other was polysorbate 60 surfactant-stabilized. When temperature increased, the fat particle packing structure inside both samples gradually decreased. The reason was that for most food emulsions, as the temperature increases, the bulk viscosity decreases, resulting in a destabilizing effect on emulsion stability.

Effect of shear rate

In order to investigate the fat particle structure variation during whipping, the effect of shear rate on fat particle structure was studied by the backlight scattering technique (Fig. 10). Both samples had the same ingredients except that one sample included caseinate (#1) and the other included Polysorbate 60 surfactant (no caseinate) (#2). With increasing shear rate, the fat particle packing structure of both samples decreased. However, the fat particle packing structure of the sample including caseinate decreased less than that of the oth-

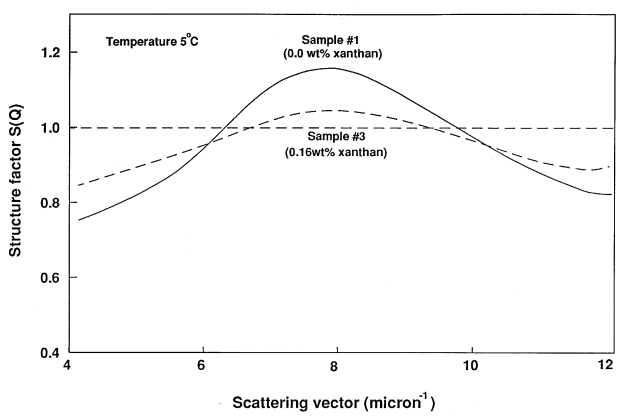

Fig. 8—Effect of xanthan on fat particle structure inside food emulsions (fat concentration: 5.14wt%).

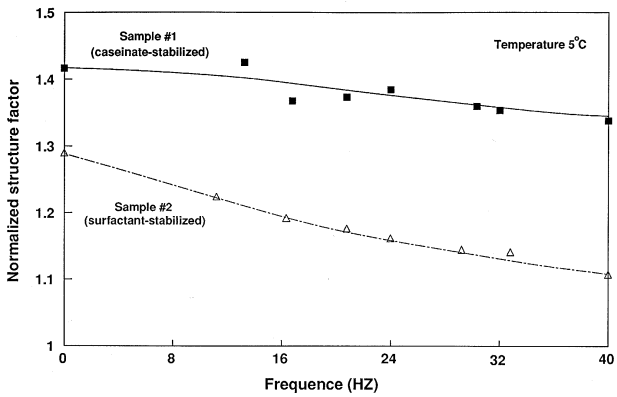

Fig. 10—Effect of shear rate on fat particle structure inside food emulsions (fat concentration: 5.14wt%).

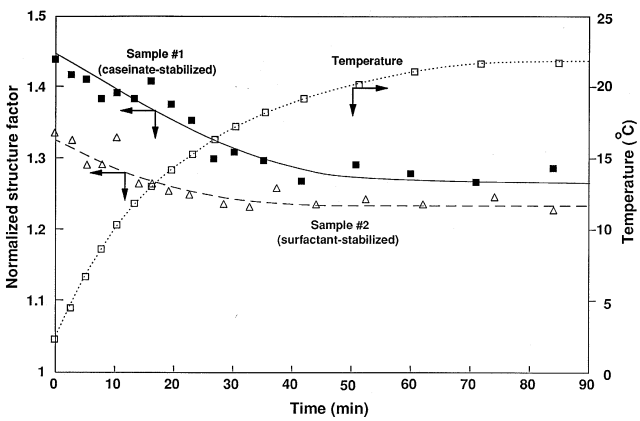

Fig. 9—Effect of temperature on fat particle structure inside food emulsions (fat concentration: 5.14wt%).

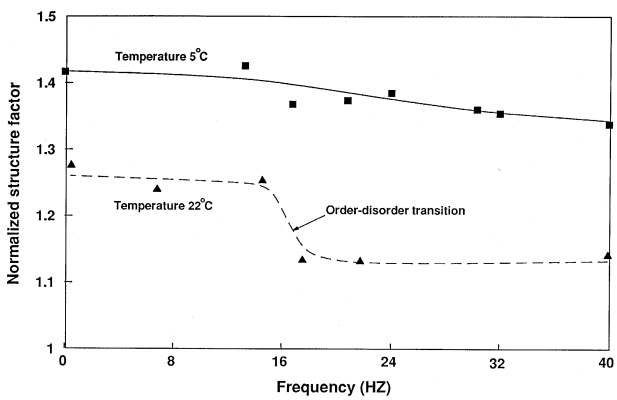

Fig. 11—Effect of shear rate on fat particle structure inside food emulsions at different temperatures (sample #1).

er sample. This was due to the fact that the microlayering formation of caseinate submicelles around fat particles helped to form an ordered fat particle structure and thereby increased the resistant force against the fat particle microstructure deformation under shear.

The effect of shear stress was determined (Fig. 11) on the fat particle structure at different temperatures. The sample (#1) included 5.14 wt% fat and 0.48 wt% caseinate. The experiment was performed at 5°C and 22°C. Increasing temperature decreased the fat particle ordering structure. Also at a high temperature (22˚C), an order-disorder transition of particle structure occurred at a frequency of 16Hz, indicating that the fat particle packing structure inside the sample collapsed. This could be explained by the combination effects of temperature and shear rate on fat particle structure. Increasing temperature decreased the fat particle packing structure as discussed. Under the shear, the deformation of the fat particle microstructure changed the relative positions of particles, therefore increased the total potential energy of the system, and produced an interparticle force tending to restore the equilibrium structure (Russel et al., 1989). This interparticle resistant force decreased with increasing temperature. Finally, at a critical shear stress, the particle structure broke at a high temperature which resulted in an order-disorder transition.

CONCLUSIONS

A NONDESTRUCTIVE METHOD OF BACKLIGHT SCATTERING to study fat particle structure in food emulsions was developed. Increasing temperature decreased the fat particle packing structure and the stability of food emulsions. Caseinate stabilized food emulsions by the formation of a caseinate adsorbed layer and by caseinate submicelle microlayering around the fat particles. Xanthan made the fat particle structure inside food emulsions less ordered, therefore it exerted an adverse effect on emulsion stability. Increasing shear rate decreased the fat particle structuring inside emulsions. At a critical shear rate, the fat particle packing structure was destroyed, and the food emulsions were destabilized. Caseinate-stabilized emulsions were much more stable than polysorbate 60-stabilized emulsions under shear.

REFERENCES

Ackerson, B. and Clark, N. 1981. Shear-induced melting. Physical Review Letters 46(2): 123.
Anderson, M. and Brooker, B. 1988. Dairy foams, in *Advances in Food Emulsions and Foams*, Elsevier Applied Science Publishers Ltd.
Brooker, B., Anderson, M., and Andrew, A. 1986. The development of structure in whipped cream. Food Microstructure 5: 277.
Brooker, B. 1990. The adsorption of crystalline fat to the air-water interface of whipped cream. Food Structure 9: 223.
Chu, X., Nikolov, A., and Wasan, D. 1996. Effects of particle size and polydispersity on the depletion and structural forces in colloidal dispersions. Langumir 12(21): 5004.
D'Aguanno, B. and Klein, R. 1991. Structural effects of polydispersity in charged colloidal dispersions. J. Chemical Society Faraday Transition 87(3): 379.
Dickinson, E. 1992. *An Introduction to Food Colloids*. Oxford University Press.
Dickinson, E. and Stainsby, G. 1988. *Advances in Food Emulsions and Foams*. Elsevier Applied Science.
Dickinson, E. and Walstra, P. 1993. *Food Colloid and Polymers: Stability and Mechanical Propertie.*. Royal Society of Chemistry, London.
Flory, P. 1956 Phase Equilibria in dolutions of rod-like particles. Proc. R. Soc. London, Ser. A 234: 73.
Flory, P. and Abe, A. 1978. Statistical thermodynamics of mixtures of rod-like particles. Macromolecules 11(6): 1119.
Hunter, R. 1987. *Foundations of Colloid Science, Volume I and Volume II*, Oxford University Press, New York.
Koczo, K., Nikolov, A., Wasan, D., Borwankar, R., and Gonsalves, A. 1996. Layering of sodium caseinate submicelles in thin liquid films - A new stability mechanism for food, Dispersions. J. Colloid & Interface Sci. 178: 694.
Koczo, K., Wasan, D., Borwankar, R., and Gonsalves, A. 1997. Flocculation of food dispersions by Gums - Isotropic/anisotropic dispersion separation by xanthan gum, Accepted for publication in Food Hydrocolloids.
Lebowitz, J. 1964. Exact solution of generalized Percus-Yevick equation for a mixture of hard sphere. Physical Review 133(4A): A895.
Mandel, F. 1971. Some remarks on the numerical evaluation of Fourier and Fourier-Bessel Transforms J. Computational Physics 7: 637.
Nieuwenhuis, E. and Vrij, A. 1979. Light scattering of PMMA latex particles in benzene: Structural Effects. J. Colloid Interface Sci. 72(2): 321.
Ornstein, L. and Zernike, F. 1914. Proc. Acad. Sci. (Amsterdam) 17: 793.
Percus, J. and Yevick, G. 1957. Physical Review 110: 1.
Russel, W., Saville, D. and Schowalter, W., 1989, Colloidal Dispersions, Cambridge University Press.
Xu, W., Nikolov, A., Wasan, D., Gonsalves, A.,and Borwankar, R., 1997, Particle Structure and Stability of Colloidal Dispersions as Probed by the Kossel Diffraction Technique, Journal of Colloid and Interface Science 191: 471.
Walstra, P., 1993, Introduction to aggregation phenomena in food colloids, in *Food Colloids and Polymers: Stability and Mechanical Properties*, The Royal Society of Chemistry.
Ms received 2/10/97; revised 9/8/97; accepted 9/20/97.

We acknowledge financial support provided by the National Science Foundation.